Electron–optical-phonon interaction in single and double heterostructures

N. Mori
Department of Electronic Engineering, Osaka University, 2-1 Yamada-oka, Suita City, Osaka 565, Japan

T. Ando
Institute for Solid State Physics, University of Tokyo, 7-22-1 Roppongi, Minato-ku, Tokyo 106, Japan
(Received 23 March 1989)

Electron–optical-phonon interactions are studied in single and double heterostructures. The Hamiltonian describing electron-phonon interactions is derived with use of orthonormal eigenmodes of phonons calculated in the dielectric continuum model. Effects of interactions are expressed in the form of an effective electron-electron interaction mediated by virtual exchange of phonons. It is given by the sum of products of coupling constants and form factors for different modes. The coupling constants correspond to the Fröhlich coupling constant in bulk and the form factors describe effects of electron confinement. The resulting expression is convenient and useful in discussing relative importance of interface modes and bulklike confined modes and also in exploring the possibility of reduction of electron–optical-phonon interactions in heterostructures. It is applied to calculations of the polaron mobility and magnetophonon resonance spectra. The results clearly demonstrate roles of interface phonons.

I. INTRODUCTION

It is well known that the mobility of a two-dimensional electron gas is enhanced considerably at low temperatures by the so-called modulation-doping technique in semiconductor heterostructures such as single heterostructures, double heterostructures (quantum wells), and superlattices. This is due to the spatial separation of electrons from donor impurities. At high temperatures, however, electron–optical-phonon interactions play a dominant role in determining various electronic properties including mobility. There have been considerable interests in the problem of the electron–optical-phonon interaction in heterostructures. As a matter of fact, there have been calculations of electron scattering rates,[1–9] two-dimensional polarons, cyclotron resonance,[10–16] hot-electron relaxation,[17] magnetophonon effects,[18–22] hot-electron magnetophonons,[23–25] etc. In most of these works, use has been made of the usual Fröhlich interaction based on bulk phonons and only effects of electron confinement have been properly taken into account. However, optical phonons can be strongly influenced by the presence of heterointerfaces as was recognized recently.[26] The purpose of the present paper is to elucidate the role of interfaces on electron–optical-phonon interactions in single and double heterostructures.

The presence of heterointerfaces gives rise to confinement of optical phonons in each layer as well as interface modes which are localized in the vicinity of interfaces. Therefore, use of the usual bulk Fröhlich Hamiltonian is certainly misleading.[27–32] It has been shown theoretically that the interface phonons can give a significant contribution to the electron–optical-phonon interaction in some cases.[27,33–37] There has been a suggestion that interactions with the confined optical phonons can be reduced in some double heterostructures in comparison with those with usual bulk phonons.[27–32] In spite of such extensive studies, effects of interfaces on electron-phonon interactions have not been fully clarified because of the inclusion of various other effects such as screening, plasmon-phonon couplings, hot phonons, etc., in most of these works.

In this paper we study the electron–optical-phonon interaction in single and double heterostructures composed of diatomic polar semiconductors (not alloys). In particular, we try to clarify roles of interface phonons as well as effects of phonon confinement on electron-phonon interactions and in which cases we can utilize the bulk Fröhlich Hamiltonian, and explore the possibility of reducing electron-phonon interactions. We proceed as follows. First, optical-phonon modes in heterostructures are determined with use of the dielectric continuum model.[38–42] Then, the Hamiltonian describing electron–optical-phonon interactions is derived by a standard quantum-mechanical method.[39,40,42] We calculate matrix elements of effective electron-electron interactions due to virtual exchange of optical phonons.[13] These matrix elements make it possible to separately discuss effects of interfaces on electron–optical-phonon interactions due to modifications of phonon modes and those due to the confinement of electron wave functions. We also consider magnetophonon effects because of the presence of a number of interesting experiments[43–54] and some remaining controversies in their explanation.

The organization of the present paper is as follows. In Sec. II we derive phonon eigenmodes and Hamiltonian for electron–optical-phonon interactions by a standard manner for the sake of completeness. In Sec. III the effective electron-electron interaction mediated by optical phonons is calculated. We show how the elec-

tron–optical-phonon interaction in heterostructures is modified relative to the case that electrons are assumed to interact with bulk longitudinal optical phonons. The resulting formula for the effective interactions is applied in actual problems in Secs. IV and V. In Sec. IV we calculate the low-field polaron mobility which is one of the best candidates to see how the electron–optical-phonon interaction is different from the case of the bulk phonons. In Sec. V the transverse magnetoresistance due to magnetophonon resonances is calculated. A summary and discussion are given in Sec. VI. Throughout this paper we set $\hbar=k_B=1$, where k_B is the Boltzmann constant.

II. INTERACTION WITH OPTICAL PHONONS

A. Dielectric continuum model

We consider single and double heterostructures whose geometry is given in Fig. 1. In the single heterostructure, there is a heterointerface normal to the z axis and the material 1 (material 2) fills up the half-space $z\geq 0$ ($z\leq 0$). In the double heterostructure, the material 1 lies between $z=\pm\frac{1}{2}a$ and the material 2 fills up the spaces $z\geq\frac{1}{2}a$ and $z\leq-\frac{1}{2}a$. In the following analysis we introduce periodic-boundary conditions in volume L^3 (i.e., $-\frac{1}{2}L\leq x,y,z\leq\frac{1}{2}L$). Optical-phonon modes in the heterostructures are determined using the classical electrostatics. For instance, we have the following equations in each layer:

$$\mathbf{P}(\mathbf{r})=\epsilon_0\chi_n(\omega)\mathbf{E}(\mathbf{r}) , \tag{2.1}$$

$$\mathbf{E}(\mathbf{r})=-\nabla\phi(\mathbf{r}) , \tag{2.2}$$

$$\nabla^2\phi(\mathbf{r})=-\frac{1}{\epsilon_0}\rho(\mathbf{r}) , \tag{2.3}$$

$$\rho(\mathbf{r})=-\nabla\cdot\mathbf{P}(\mathbf{r}) , \tag{2.4}$$

together with conventional boundary conditions at heterointerface(s), where $\mathbf{r}$ is the three-dimensional position vector, $\mathbf{P}(\mathbf{r})$ the polarization field, $\mathbf{E}(\mathbf{r})$ the electric field, $\phi(\mathbf{r})$ the scalar potential, $\rho(\mathbf{r})$ the total charge density, ϵ_0 the permittivity of vacuum, and $\chi_n(\omega)=\epsilon_n(\omega)-1$ the dielectric susceptibility of the material n ($n=1,2$). The dielectric function $\epsilon_n(\omega)$ is given by

$$\epsilon_n(\omega)=\kappa_{\infty n}\frac{\omega^2-\omega_{\mathrm{L}n}^2}{\omega^2-\omega_{\mathrm{T}n}^2} , \tag{2.5}$$

where $\omega_{\mathrm{L}n}$ and $\omega_{\mathrm{T}n}$ are the frequency of longitudinal-optical (LO) phonon and the transverse-optical (TO) phonon, respectively, and $\epsilon_0\kappa_{\infty n}$ is the high-frequency dielectric constant. Because of the translational invariance along the interface, we can introduce two-dimensional Fourier transforms along the xy plane and work in $(\mathbf{Q},z)$ space, where $\mathbf{Q}$ is the two-dimensional wave vector. Moreover we choose the x axis in the direction of the $\mathbf{Q}$ vector for the sake of simplicity. Working on this coordinates system in Eqs. (2.1)–(2.4); we can separate the polarization field into an s-polarization part $[\mathbf{P}(\mathbf{Q},z)=(0,P_y,0)]$ and a p-polarization part $[\mathbf{P}(\mathbf{Q},z)=(P_x,0,P_z)]$, which are completely decoupled. Since electrons do not couple to phonons with s polarization, we will consider only p polarization in the following analysis.

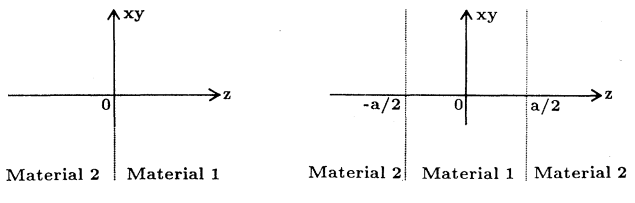

(a) Single Heterostructure (b) Double Heterostructure

FIG. 1. Geometry relevant to the discussion of the single (a) and double heterostructure (b). In the single heterostructure, material 1 and 2 fill up the right ($z\geq 0$) and the left ($z\leq 0$) half-space, respectively. In the double heterostructure, material 1 lies between $z=\pm\frac{1}{2}a$ (a is the well width) with heterointerfaces normal to z axis and material 2 fills up the half-spaces $z\geq\frac{1}{2}a$ and $z\leq-\frac{1}{2}a$.

B. Equation of motion and normal modes

We can readily solve the eigenequation for $\mathbf{P}(\mathbf{Q},z)$, which is obtained from Eqs. (2.1)–(2.4) by the two dimensional Fourier transforms. The eigenmodes $\mathbf{P}^{(J)}(\mathbf{Q},z)$ (J is a quantum number) are determined in such a way that the corresponding relative displacements of the positive and negative ions are orthonormalized. We have

$$\int_{-L/2}^{+L/2}dz[(\epsilon_0 n_n\mu_n)^{1/2}\mathbf{u}^{(J)}(\mathbf{Q},z)]^*\cdot[(\epsilon_0 n_n\mu_n)^{1/2}\mathbf{u}^{(I)}(\mathbf{Q},z)]=\delta_{IJ} , \tag{2.6}$$

where $\mathbf{u}(\mathbf{Q},z)$ is the two-dimensional Fourier transform of the relative displacement of the ion pair, n_n the number of ion pairs per unit volume, and μ_n the reduced mass of the ion pair. The relation between $\mathbf{P}(\mathbf{r})$ and $\mathbf{u}(\mathbf{r})$ is given by the equation of motion

$$-\mu_n\omega^2\mathbf{u}(\mathbf{r})=-\mu_n\omega_{0n}^2\mathbf{u}(\mathbf{r})+e_n^*\mathbf{E}_{\mathrm{loc}}(\mathbf{r}) \tag{2.7}$$

and the microscopic relation

$$\mathbf{P}(\mathbf{r})=n_n e_n^*\mathbf{u}(\mathbf{r})+n_n a_n\mathbf{E}_{\mathrm{loc}}(\mathbf{r}) , \tag{2.8}$$

where ω_{0n} is the frequency associated with short-range forces between ions, e_n^* is the effective charge of the ions, and a_n is the electronic polarizability per ion pair. The local field $\mathbf{E}_{\mathrm{loc}}(\mathbf{r})$ satisfies the well-known Lorentz relation $\mathbf{E}_{\mathrm{loc}}=\mathbf{E}+\mathbf{P}/3\epsilon_0$.

The obtained eigenmodes in single and double heterostructures are summarized in Tables I and II, respectively. Those eigenmodes are exact in the limit of $L\rightarrow+\infty$. We have shown only the x components in case of double heterostructures for conciseness. (It is straightforward to calculate the z components from the x components using the relations in each layer: $\partial P_x/\partial x=iQP_z$ if $\omega\neq\omega_{\mathrm{T}n}$ and/or $\partial P_z/\partial z=-iQP_x$ if $\omega\neq\omega_{\mathrm{L}n}$.) Those eigenmodes satisfy the closure relation:

$$\sum_J [(\epsilon_0 n_{n'}\mu_{n'})^{1/2} u_\alpha^{(J)}(\mathbf{Q},z')]^* [(\epsilon_0 n_n \mu_n)^{1/2} u_\alpha^{(J)}(\mathbf{Q},z)]$$

$$= \delta(z-z') \quad (\alpha = x \text{ or } z) . \tag{2.9}$$

There are three types of modes in the single heterostructure. (1) *Interface modes* whose amplitude decreases exponentially away from the interface. (2) *Half-space LO modes* which have the frequency ω_{Ln} of bulk LO phonons and no polarization in the opposite layer and whose polarization parallel to the interface vanishes at the interface. (3) *Half-space TO modes* which have frequency ω_{Tn} of bulk TO phonons and no polarization in the opposite layer and whose polarization field normal to the interface has a node at the interface. The frequencies of the interface modes, $\omega_\pm$, are given by the solutions of

$$\epsilon_1(\omega)+\epsilon_2(\omega)=0 . \tag{2.10}$$

These frequencies lie between ω_{Tn} and ω_{Ln}. For example, when we set $\omega_{L1}=36.2$ meV, $\omega_{T1}=33.3$ meV, $\kappa_{\infty 1}=10.9$, $\omega_{L2}=50.1$ meV, $\omega_{T2}=44.8$ meV, and $\kappa_{\infty 2}=8.16$, which are the relevant physical parameters for a GaAs/AlAs single heterostructure, we get $\omega_+=47.4$ meV and $\omega_-=34.6$ meV.

There are six types of modes in the double heterostructure. (1) *Symmetric interface modes* whose amplitude decreases away from the interfaces and whose polarization field parallel to the interfaces is symmetric with respect to $z=0$. (2) *Antisymmetric interface modes* whose amplitude decreases away from the interfaces and whose polarization field parallel to the interfaces is antisymmetric with respect to $z=0$. (3) *Confined LO modes* with frequency ω_{L1}, which have vanishing polarization field in the barrier layers and whose polarization field parallel to the interfaces has nodes at the interfaces. (4) *Confined TO modes* with frequency ω_{T1}, which have vanishing polarization field in the barrier layers and whose polarization field normal to the interfaces has nodes at the interfaces. (5) *Half-space LO modes* in the barrier layers. (6) *Half-space TO modes* in the barrier layers.

The frequencies of the symmetric interface modes, $\omega_{S\pm}$, are given by the solutions of

$$\epsilon_1(\omega)\tanh(\tfrac{1}{2}Qa)+\epsilon_2(\omega)=0 . \tag{2.11}$$

For short wavelengths $\omega_{S\pm}$ approaches $\omega_\pm$ and for long wavelengths it approaches ω_{L2} or ω_{T1}. The frequencies of the antisymmetric interface modes, $\omega_{A\pm}$, are similarly given by

$$\epsilon_1(\omega)\coth(\tfrac{1}{2}Qa)+\epsilon_2(\omega)=0 . \tag{2.12}$$

For short wavelengths $\omega_{A\pm}$ approaches $\omega_\pm$ and for long wavelengths it approaches ω_{L1} or ω_{T2}. In Fig. 2 we show $\omega_{S\pm}$ and $\omega_{A\pm}$ in an AlAs/GaAs/AlAs double heterostructure as a function of Qa.

TABLE I. The p-polarization eigenmodes in single heterostructures.

Mode Eigenfrequency	Eigenvector
Interface mode[a]	
$\omega_\pm$	$\left.\begin{matrix}P_x(\mathbf{Q},z)\\P_z(\mathbf{Q},z)\end{matrix}\right\} = \left[\frac{\theta_1(\omega_\pm)\chi_1^2(\omega_\pm)}{\omega_{p1}^2}+\frac{\theta_2(\omega_\pm)\chi_2^2(\omega_\pm)}{\omega_{p2}^2}\right]^{-1/2} \chi_n(\omega_\pm)\sqrt{Q}\,e^{-Q\lvert z\rvert}\times \begin{cases} i \\ -\mathrm{sgn}(z)\end{cases}$, where $n=\begin{cases}1 & \text{if } z\geq 0\\ 2, & \text{if } z<0\end{cases}$, $\omega_{pn}=\frac{n_n e_n^{*2}}{\epsilon_0\mu_n}$ and $\theta_n(\omega)=\left[1+(\omega_{0n}^2-\omega^2)\frac{n_n a_n}{\epsilon_0\omega_{pn}^2}\right]^{-2}$
Half-space LO mode	
ω_{Ln}	$\left.\begin{matrix}P_x(\mathbf{Q},z)\\P_z(\mathbf{Q},z)\end{matrix}\right\} = \frac{2}{\sqrt{L}}\frac{\omega_{pn}}{\theta_n^{1/2}(\omega_{Ln})}\frac{1}{(Q^2+q_z^2)^{1/2}}\mathsf{H}_n(z)\times \begin{cases} iQ\sin(q_z z) \\ q_z\cos(q_z z)\end{cases}$ $(q_z>0)^b$, where $\mathsf{H}_n(z)=\begin{cases}1 & \text{if } z \text{ is in the } n \text{ layer}\\ 0 & \text{otherwise}\end{cases}$
Half-space TO mode	
ω_{Tn}	$\left.\begin{matrix}P_x(\mathbf{Q},z)\\P_z(\mathbf{Q},z)\end{matrix}\right\} = \frac{2}{\sqrt{L}}\frac{\omega_{pn}}{\theta_n^{1/2}(\omega_{Tn})}\frac{1}{(Q^2+q_z^2)^{1/2}}\mathsf{H}_n(z)\times \begin{cases} iq_z\cos(q_z z) \\ Q\sin(q_z z)\end{cases}$ $(q_z>0)^b$

[a]The frequencies $\omega_\pm$ are the solutions of $\epsilon_1(\omega)+\epsilon_2(\omega)=0$.
[b]$q_z=(2\pi/L)m$ $(m=1,2,3,\ldots)$.

TABLE II. The p-polarization eigenmodes in double heterostructures.

Mode Eigenfrequency	Eigenvector
Symmetric interface mode[a] $\omega_{S\pm}$	$P_x(\mathbf{Q},z)=i\left[\frac{\theta_1(\omega_{S\pm})\chi_1^2(\omega_{S\pm})}{\omega_{p1}^2}\tanh(\frac{1}{2}Qa)+\frac{\theta_2(\omega_{S\pm})\chi_2^2(\omega_{S\pm})}{\omega_{p2}^2}\right]^{-1/2}\chi_n(\omega_{S\pm})\left[\frac{Q}{2}\right]^{1/2}f_S(Qz)$, where $n=\begin{cases}1 & \text{if } -\frac{1}{2}a\le z\le\frac{1}{2}a\\ 2 & \text{otherwise}\end{cases}$
Antisymmetric interface mode[b] $\omega_{A\pm}$	$P_x(\mathbf{Q},z)=i\left[\frac{\theta_1(\omega_{A\pm})\chi_1^2(\omega_{A\pm})}{\omega_{p1}^2}\coth(\frac{1}{2}Qa)+\frac{\theta_2(\omega_{A\pm})\chi_2^2(\omega_{A\pm})}{\omega_{p2}^2}\right]^{-1/2}\chi_n(\omega_{A\pm})\left[\frac{Q}{2}\right]^{1/2}f_A(Qz)$, where $n=\begin{cases}1 & \text{if } -\frac{1}{2}a\le z\le\frac{1}{2}a\\ 2 & \text{otherwise}\end{cases}$
Confined LO mode ω_{L1}	$P_x(\mathbf{Q},z)=i\left[\frac{2}{a}\right]^{1/2}\frac{\omega_{p1}}{\theta_1^{1/2}(\omega_{L1})}\frac{Q}{(Q^2+q_z^2)^{1/2}}H_C(z)\times\begin{cases}\cos\left[\frac{m\pi}{a}z\right], & m=1,3,5,\ldots\\ \sin\left[\frac{m\pi}{a}z\right], & m=2,4,6,\ldots\end{cases}$, where $H_C(z)=\begin{cases}1 & \text{if } -\frac{1}{2}z\le z\le\frac{1}{2}a\\ 0 & \text{otherwise}\end{cases}$
Confined TO mode ω_{T1}	$P_x(\mathbf{Q},z)=i\left[\frac{2}{a}\right]^{1/2}\frac{\omega_{p1}}{\theta_1^{1/2}(\omega_{T1})}\frac{q_z}{(Q^2+q_z^2)^{1/2}}H_C(z)\times\begin{cases}\sin\left[\frac{m\pi}{a}z\right], & m=1,3,5,\ldots\\ \cos\left[\frac{m\pi}{a}z\right], & m=2,4,6,\ldots\end{cases}$
Half-space LO mode[c] ω_{L2}	$P_{x,\pm}(\mathbf{Q},z)=i\frac{2}{\sqrt{L}}\frac{\omega_{p2}}{\theta_2^{1/2}(\omega_{L2})}\frac{Q}{(Q^2+q_z^2)^{1/2}}H_{H\pm}(z)\sin[q_z(z\mp\frac{1}{2}a)]$ $(q_z>0)$[d], where $H_{H+}(z)=\begin{cases}1 & \text{if } z\ge\frac{1}{2}a\\ 0 & \text{otherwise}\end{cases}$ and $H_{H-}(z)=\begin{cases}1 & \text{if } z\le-\frac{1}{2}a\\ 0 & \text{otherwise}\end{cases}$
Half-space TO mode[c] ω_{T2}	$P_{x,\pm}(\mathbf{Q},z)=i\frac{2}{\sqrt{L}}\frac{\omega_{p2}}{\theta_2^{1/2}(\omega_{T2})}\frac{q_z}{(Q^2+q_z^2)^{1/2}}H_{H\pm}(z)\cos[q_z(z\mp\frac{1}{2}a)]$ $(q_z>0)$[d]

[a]The frequencies $\omega_{S\pm}$ are the solutions of $\epsilon_1(\omega)\tanh(\frac{1}{2}Qa)+\epsilon_2(\omega)=0$, and the function $f_S(Qz)$ is defined in the text.
[b]The frequencies $\omega_{A\pm}$ are the solutions of $\epsilon_1(\omega)\coth(\frac{1}{2}Qa)+\epsilon_2(\omega)=0$, and the function $f_A(Qz)$ is defined in the text.
[c]$P_{x,+}$ ($P_{x,-}$) is the polarization eigenvector for the half-space mode of $z\ge\frac{1}{2}a$ ($z\le-\frac{1}{2}a$).
[d]$q_z=(2\pi/L)m$ ($m=1,2,3,\ldots$).

TABLE III. The electron–optical-phonon interaction Hamiltonian in single heterostructures.

Optical-phonon mode	Interaction Hamiltonian
Interface mode[a]	$\mathcal{H}_{\mathrm{ep},\pm}=\sum_{\mathbf{Q}}\left[\frac{\omega_{\pm}e^2}{2\epsilon_0 L^2}\right]^{1/2}\left[\frac{2}{\beta_1^{-1}(\omega_{\pm})+\beta_2^{-1}(\omega_{\pm})}\right]^{1/2}\frac{1}{\sqrt{2Q}}e^{i\mathbf{Q}\cdot\mathbf{R}}e^{-Q\lvert z\rvert}\,[a_{\pm}(\mathbf{Q})+a_{\pm}^{\dagger}(-\mathbf{Q})]$
Half-space LO mode	$\mathcal{H}_{\mathrm{ep},n}=-\sum_{q_z>0}\sum_{\mathbf{Q}}\left[\frac{\omega_{\mathrm{L}n}e^2}{2\epsilon_0 L^3}\right]^{1/2}\left[\frac{1}{\kappa_{\infty n}}-\frac{1}{\kappa_{0n}}\right]^{1/2}\frac{1}{(Q^2+q_z^2)^{1/2}}e^{i\mathbf{Q}\cdot\mathbf{R}}\,\mathsf{H}_n(z)2\sin(q_z z)\times[a_{n,q_z}(\mathbf{Q})+a_{n,q_z}^{\dagger}(-\mathbf{Q})]$

[a]The function $\beta_n(\omega)$ is defined in the text.

C. Electron–optical-phonon Hamiltonian

Since the interaction energy of an electron at the position $\mathbf{r}$ with the polarization field is given by $-e\phi(\mathbf{r})$, we can determine the electron–optical-phonon interaction Hamiltonian by expanding the scalar potential in terms of the normal modes obtained above. The resulting interaction Hamiltonian in single and double heterostructures are given in Tables III and IV, respectively. Note that phonons with the bulk TO-phonon frequency do not couple to electrons.

III. EFFECTIVE ELECTRON-ELECTRON INTERACTION

A. Single heterostructures

It is very convenient and useful to define the two-dimensional effective electron-electron interaction due to exchange of optical phonons.[13] The effective electron-electron interaction can be formally written in the same form for each phonon mode j. We have

TABLE IV. The electron–optical-phonon interaction Hamiltonian in double heterostructures.

Optical-phonon mode	Interaction Hamiltonian
Symmetric interface mode	$\mathcal{H}_{\mathrm{ep},S\pm}=\sum_{\mathbf{Q}}\left[\frac{\omega_{S\pm}e^2}{2\epsilon_0 L^2}\right]^{1/2}[\beta_1^{-1}(\omega_{S\pm})\tanh(\tfrac{1}{2}Qa)+\beta_2^{-1}(\omega_{S\pm})]^{-1/2}\frac{1}{\sqrt{2Q}}e^{i\mathbf{Q}\cdot\mathbf{R}}f_S(Q,z)\times[a_{S\pm}(\mathbf{Q})+a_{S\pm}^{\dagger}(-\mathbf{Q})]$
Antisymmetric interface mode	$\mathcal{H}_{\mathrm{ep},A\pm}=\sum_{\mathbf{Q}}\left[\frac{\omega_{A\pm}e^2}{2\epsilon_0 L^2}\right]^{1/2}[\beta_1^{-1}(\omega_{A\pm})\coth(\tfrac{1}{2}Qa)+\beta_2^{-1}(\omega_{A\pm})]^{-1/2}\frac{1}{\sqrt{2Q}}e^{i\mathbf{Q}\cdot\mathbf{R}}f_A(Qz)\times[a_{A\pm}(\mathbf{Q})+a_{A\pm}^{\dagger}(-\mathbf{Q})]$
Confined LO mode	$\mathcal{H}_{\mathrm{ep},C}=-\sum_{m=1,3,5,\ldots}\sum_{\mathbf{Q}}\left[\frac{\omega_{\mathrm{L}1}e^2}{2\epsilon_0 L^2}\right]^{1/2}\left[\frac{1}{\kappa_{\infty 1}}-\frac{1}{\kappa_{01}}\right]^{1/2}\left[\frac{2}{a}\right]^{1/2}\frac{1}{[Q^2+(m\pi/a)^2]^{1/2}}e^{i\mathbf{Q}\cdot\mathbf{R}}\times\mathsf{H}_C(z)\cos\left[\frac{m\pi}{a}z\right][a_m(\mathbf{Q})+a_m^{\dagger}(-\mathbf{Q})]$ $-\sum_{m=2,4,6,\ldots}\sum_{\mathbf{Q}}\left[\frac{\omega_{\mathrm{L}1}e^2}{2\epsilon_0 L^2}\right]^{1/2}\left[\frac{1}{\kappa_{\infty 1}}-\frac{1}{\kappa_{01}}\right]^{1/2}\left[\frac{2}{a}\right]\frac{1}{[Q^2+(m\pi/a)^2]^{1/2}}e^{i\mathbf{Q}\cdot\mathbf{R}}\times\mathsf{H}_C(z)\sin\left[\frac{m\pi}{a}z\right][a_m(\mathbf{Q})+a_m^{\dagger}(-\mathbf{Q})]$
Half-space LO mode	$\mathcal{H}_{\mathrm{ep},H\pm}=-\sum_{q_z>0}\sum_{\mathbf{Q}}\left[\frac{\omega_{\mathrm{L}2}e^2}{2\epsilon_0 L^3}\right]^{1/2}\left[\frac{1}{\kappa_{\infty 2}}-\frac{1}{\kappa_{02}}\right]^{1/2}\frac{1}{(Q^2+q_z^2)^{1/2}}e^{i\mathbf{Q}\cdot\mathbf{R}}\times\mathsf{H}_{H\pm}(z)2\sin[q_z(z\mp\tfrac{1}{2}a)][a_{H\pm,q_z}(\mathbf{Q})+a_{H\pm,q_z}^{\dagger}(-\mathbf{Q})]$

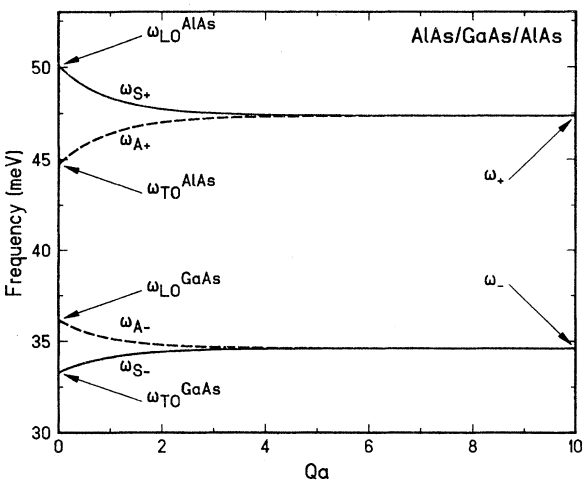

FIG. 2. Frequencies of symmetric and antisymmetric interface phonons as a function Qa (Q is the magnitude of phonon wave vector parallel to the interfaces) for an AlAs/GaAs/AlAs double heterostructure. The symmetric (antisymmetric) interface phonons $\omega_{S\pm}$ ($\omega_{A\pm}$) converge to $\omega_\pm$ (the interface phonons of a GaAs/AlAs single heterostructure) as $Qa\to+\infty$. At $Qa=0$, $\omega_{S+}=\omega_{L2}$, $\omega_{S-}=\omega_{T1}$, $\omega_{A+}=\omega_{T2}$, and $\omega_{A-}=\omega_{L1}$.

$$V_j(\mathbf{Q},i\nu_m)=2\pi\alpha_j\left[\frac{2\omega_j^3}{m^*}\right]^{1/2}\frac{1}{2Q}F_j(Q)D_j(i\nu_m)\ , \tag{3.1}$$

where α_j is the coupling constant, $F_j(Q)$ is the form factor, $D_j(i\nu_m)=2\omega_j/[(i\nu_m)^2-\omega_j^2]$ is the phonon Green's function with imaginary frequency $i\nu_m$, ω_j is the eigenfrequency, m^* is an electron effective mass, and we have set $L=1$. In general the effective electron-electron interaction depends on four electron subband indices s_1,s_2,s_3,s_4.[13] For the sake of simplicity, in the following analysis we confine ourselves to the ground subband ($s_1=s_2=s_3=s_4=0$). In Eq. (3.1), α_j is defined as the term independent of the electron wave function $\xi_0(z)$ associated with the quantized z motion and reduces to the usual bulk Fröhlich coupling constant if the difference between materials 1 and 2 is neglected, and the form factor $F_j(Q)$ is defined as the term that is independent of material parameters (such as $\omega_{Ln},\omega_{Tn},\kappa_{\infty n}$, etc.).

1. Coupling constant α_j

The coupling constants of the half-space LO phonons are given by

$$\alpha_n=\frac{e^2}{4\pi\epsilon_0}\left[\frac{m^*}{2\omega_{Ln}}\right]^{1/2}\left[\frac{1}{\kappa_{\infty n}}-\frac{1}{\kappa_{0n}}\right]\quad(n=1,2)\ , \tag{3.2}$$

with $\kappa_{0n}=(\omega_{Ln}/\omega_{Tn})^2\kappa_{\infty n}$. It is identical to the Fröhlich coupling constant for the bulk material n. On the other hand, the coupling constants of the interface phonons are given by

$$\alpha_\pm=\frac{e^2}{4\pi\epsilon_0}\left[\frac{m^*}{2\omega_\pm}\right]^{1/2}\frac{2}{\beta_1^{-1}(\omega_\pm)+\beta_2^{-1}(\omega_\pm)}\ , \tag{3.3}$$

with

$$\beta_n(\omega)=\left[\frac{1}{\kappa_{\infty n}}-\frac{1}{\kappa_{0n}}\right]\frac{\omega_{Ln}^2}{\omega^2}\left[\frac{\omega^2-\omega_{Tn}^2}{\omega_{Ln}^2-\omega_{Tn}^2}\right]^2\ . \tag{3.4}$$

Since $\alpha_\pm$ is proportional to the harmonic mean of $\beta_1(\omega_\pm)$ and $\beta_2(\omega_\pm)$, it is almost determined by the smaller value of $\beta_1(\omega_\pm)$ and $\beta_2(\omega_\pm)$. The function $\beta_n(\omega)$, which becomes $(1/\kappa_{\infty n}-1/\kappa_{0n})$ at $\omega=\omega_{Ln}$ and 0 at $\omega=\omega_{Tn}$, describes effects of the shift of the eigenfrequency on the coupling constant. Since $\omega_\pm$ lies between ω_{Tn} and ω_{Ln}, where $\beta_n(\omega)$ is always smaller than $(1/\kappa_{\infty n}-1/\kappa_{0n})$, $\alpha_\pm$ cannot become extremely larger than the usual bulk Fröhlich coupling constant. For example, in GaAs/AlAs heterostructures, we get $\alpha_1=0.071$, $\alpha_2=0.11$, $\alpha_+=0.054$, and $\alpha_-=0.031$, when we set $m^*=0.067m_0$.

2. Form factor $F_j(Q)$

In single heterostructures the form factors are given by

$$F_I(Q)=\left[\int_{-\infty}^{+\infty}dz\,|\xi_0(z)|^2e^{-Q|z|}\right]^2\ , \tag{3.5}$$

$$F_{H+}(Q)=\int_0^{+\infty}dz\int_0^{+\infty}dz'\,|\xi_0(z)|^2\,|\xi_0(z')|^2\times(e^{-Q|z-z'|}-e^{-Q|z+z'|})\ , \tag{3.6}$$

$$F_{H-}(Q)=\int_{-\infty}^{0}dz\int_{-\infty}^{0}dz'\,|\xi_0(z)|^2\,|\xi_0(z')|^2\times(e^{-Q|z-z'|}-e^{-Q|z+z'|})\ , \tag{3.7}$$

where $F_I(Q)$ is for interface phonons (ω_+ or ω_-), $F_{H+}(Q)$ is for the half-space phonons in the right half-space (ω_{L1}), and $F_{H-}(Q)$ is in the left half-space (ω_{L2}). These form factors always satisfy the relation

$$F_B(Q)=F_I(Q)+F_{H+}(Q)+F_{H-}(Q)\ , \tag{3.8}$$

independently of $\xi_0(z)$, where $F_B(Q)$ is the form factor in the case that electrons are assumed to interact with bulk LO phonons, given by

$$F_B(Q)=\int_{-\infty}^{+\infty}dz\int_{-\infty}^{+\infty}dz'\,|\xi_0(z)|^2\,|\xi_0(z')|^2\,e^{-Q|z-z'|}\ . \tag{3.9}$$

This *sum rule* is a direct consequence of the complete orthonormality of the eigenmodes $\mathbf{u}^{(J)}(\mathbf{r})$ and is a major advantage of considering the effective electron-electron interaction. If we neglect the difference in eigenfrequencies due to the existence of the interface, namely, if we neglect the difference in coupling constants of phonon modes, the effective electron-electron interaction is the same as that for bulk phonons.

Let us use the Fang-Howard trial function[55]

$$\xi_0(z)=\left[\frac{b^3}{2}\right]^{1/2}z\exp(-\tfrac{1}{2}bz)\quad\text{for } z\geq0\ . \tag{3.10}$$

In Fig. 3 we show $F_I(Q)$ and $F_{H+}(Q)$ as a function of Q/b together with $F_B(Q)$ for comparison. Since we use the wave function which vanishes in the left half-space, $F_{H-}(Q)$ is always equal to zero. For long wavelengths or

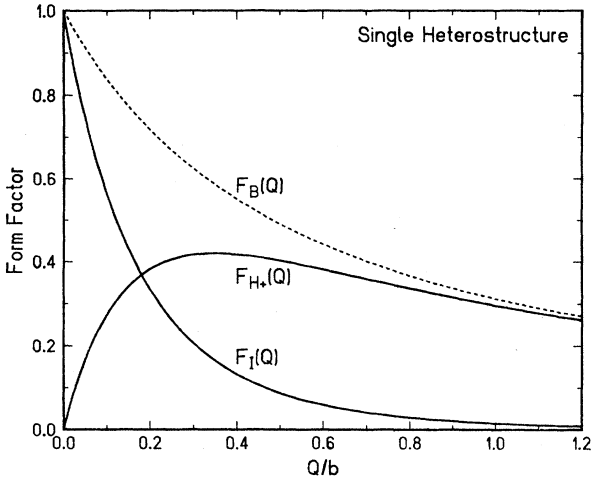

FIG. 3. The form factors in a single heterostruture as a function of Q/b [b is the Fang-Howard trial parameter (Ref. 55)]. $F_I(Q)$ is for interface phonons, $F_{H+}(Q)$ for half-space phonons, and $F_B(Q)$ for bulk phonons. Since the electron wave function vanishes for $z<0$, $F_{H-}(Q)$ is identically zero, and $F_I(Q)+F_{H+}(Q)=F_B(Q)$.

short average distances between electrons and the interface (i.e., $Q/b\rightarrow 0$), $F_I(Q)$ increases and approaches $F_B(Q)$, because the scalar potential associated with the interface phonons decreases exponentially away from the interface according to $\exp(-Q|z|)$. On the other hand, $F_{H+}(Q)$ approaches $F_B(Q)$ for short wavelengths or long average distances between electrons and the interface as is expected. For a fixed wavelength, the average distance between electrons and the interface determines the ratio of the contribution of the interface phonons to the total electron–optical-phonon interaction.

B. Double heterostructures

The effective electron-electron interaction is given by the same expression as Eq. (3.1).

1. Coupling constant $\alpha_j(Q)$

The coupling constants of the confined phonons α_1 and that of the half-space phonons in barrier layers α_2 are also identical to the bulk Fröhlich coupling constants, and given by Eq. (3.2). Since the eigenfrequencies of interfaces phonons have dispersion, the coupling constants depend on Q. Those of the symmetric interface phonons with frequency $\omega_{S\pm}$ are written as

$$\alpha_{S\pm}(Q)=\frac{e^2}{4\pi\epsilon_0}\left[\frac{m^*}{2\omega_{S\pm}}\right]^{1/2}\times\frac{\tanh(\frac{1}{2}Qa)+1}{\beta_1^{-1}(\omega_{S\pm})\tanh(\frac{1}{2}Qa)+\beta_2^{-1}(\omega_{S\pm})}\ . \tag{3.11}$$

For short wavelengths or wide well widths ($Qa\rightarrow+\infty$), $\alpha_{S\pm}(Q)$ approaches $\alpha_\pm$, which is the coupling constant in the single heterostructure. This is because the exponential decay of the scalar potential associated with the interface phonons implies decreasing influence of the two interfaces as decreasing wavelength or increasing well width. For long wavelengths or narrow well widths ($Qa\rightarrow 0$) the frequency of symmetry interface phonons approaches the TO-phonon frequency of the well layer, ω_{T1}, or the LO-phonon frequency of the barrier layers, ω_{L2}, resulting in the coupling constants approaching 0 or α_2 (the Fröhlich coupling constant of the barrier's material). In Fig. 4 we show the coupling constants of interface phonons as a function of Qa for an AlAs/GaAs/AlAs double heterostructure.

The coupling constants of antisymmetric interface phonons with frequency $\omega_{A\pm}$ are written as

$$\alpha_{A\pm}(Q)=\frac{e^2}{4\pi\epsilon_0}\left[\frac{m^*}{2\omega_{A\pm}}\right]^{1/2}\times\frac{\coth(\frac{1}{2}Qa)+1}{\beta_1^{-1}(\omega_{A\pm})\coth(\frac{1}{2}Qa)+\beta_2^{-1}(\omega_{A\pm})}\ . \tag{3.12}$$

It is readily seen that $\alpha_{A\pm}(Q)$ converges to $\alpha_\pm$, which is the coupling constant in single heterostructures, for short wavelengths or wide well widths, and it approaches α_1 (the Fröhlich coupling constant of the well's material) or 0 for long wavelengths or narrow well widths (Fig. 4).

2. Form factor $F_j(Q)$

The form factors for the ground subband are given by

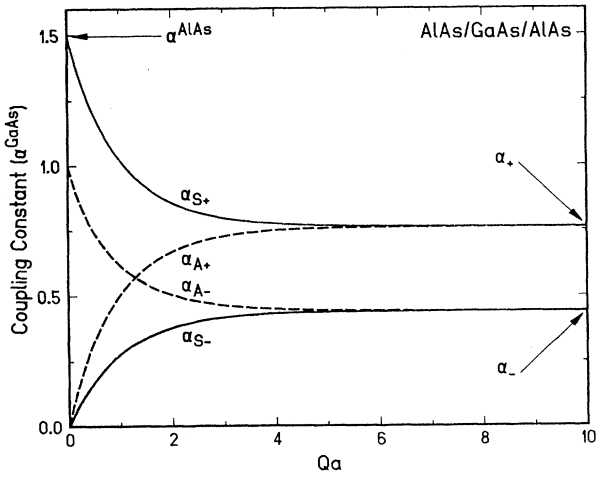

FIG. 4. Coupling constants of the symmetric $\alpha_{S\pm}(Q)$ and antisymmetric $\alpha_{A\pm}(Q)$ interface phonons as a function Qa for an AlAs/GaAs/AlAs double heterostructure. $\alpha_{S\pm}(Q)$ [$\alpha_{A\pm}(Q)$] converges to $\alpha_\pm$ as $Qa\rightarrow+\infty$. At $Qa=0$, $\alpha_{S+}=\alpha_2$, $\alpha_{S-}=0$, $\alpha_{A+}=0$, and $\alpha_{A-}=\alpha_1$.

$$F_S(Q)=\frac{1}{1+\tanh(\frac{1}{2}Qa)}\left[\int_{-\infty}^{+\infty}dz\,|\xi_0(z)|^2 f_S(Qz)\right]^2, \tag{3.13}$$

$$F_A(Q)=\frac{1}{1+\coth(\frac{1}{2}Qa)}\left[\int_{-\infty}^{+\infty}dz\,|\xi_0(z)|^2 f_A(Qz)\right]^2, \tag{3.14}$$

$$F_C(Q)=\int_{-a/2}^{a/2}dz\int_{-a/2}^{a/2}dz'\,|\xi_0(z)|^2\,|\xi_0(z')|^2\left[e^{-Q|z-z'|}-\frac{1}{1+\tanh(\frac{1}{2}Qa)}\frac{\cosh(Qz)\cosh(Qz')}{\cosh^2(\frac{1}{2}Qa)}-\frac{1}{1+\coth(\frac{1}{2}Qa)}\frac{\sinh(Qz)\sinh(Qz')}{\sinh^2(\frac{1}{2}Qa)}\right], \tag{3.15}$$

$$F_{H+}(Q)=\int_{a/2}^{+\infty}dz\int_{a/2}^{+\infty}dz'\,|\xi_0(z)|^2\,|\xi_0(z')|^2(e^{-Q|z-z'|}-e^{-Q|z+z'-a|}), \tag{3.16}$$

$$F_{H-}(Q)=\int_{-\infty}^{-a/2}dz\int_{-\infty}^{-a/2}dz'\,|\xi_0(z)|^2\,|\xi_0(z')|^2(e^{-Q|z-z'|}-e^{-Q|z+z'+a|}), \tag{3.17}$$

where $F_S(Q)$ is for symmetric interface phonons (ω_{S+} or ω_{S-}), $F_A(Q)$ is for antisymmetric interface phonons (ω_{A+} or ω_{A-}), $F_C(Q)$ is for the confined phonons (ω_{L1}), $F_{H+}(Q)$ is for the half-space phonons (ω_{L2}) in the barrier layer $z\geq\frac{1}{2}a$, and $F_{H-}(Q)$ is for the half-space phonons (ω_{L2}) in the barrier layer $z\leq-\frac{1}{2}a$. The functions $f_S(Qz)$ and $f_A(Qz)$ are defined as

$$f_S(Qz)=\begin{cases}e^{Q(z+\frac{1}{2}a)}, & z\leq-\frac{1}{2}a\\ \cosh(Qz)/\cosh(\frac{1}{2}Qa), & -\frac{1}{2}a\leq z\leq\frac{1}{2}a\\ e^{-Q(z-\frac{1}{2}a)}, & z\geq\frac{1}{2}a\end{cases} \tag{3.18}$$

$$f_A(Qz)=\begin{cases}-e^{Q(z+\frac{1}{2}a)}, & z\leq-\frac{1}{2}a\\ \sinh(Qz)/\sinh(\frac{1}{2}Qa), & -\frac{1}{2}a\leq z\leq\frac{1}{2}a\\ e^{-Q(z-\frac{1}{2}a)}, & z\geq\frac{1}{2}a\ .\end{cases} \tag{3.19}$$

These form factors also satisfy the *sum rule* independently of $\xi_0(z)$, that is

$$F_B(Q)=F_S(Q)+F_A(Q)+F_C(Q)+F_{H+}(Q)+F_{H-}(Q)\ , \tag{3.20}$$

where the function $F_B(Q)$ is given by Eq. (3.9).

For the sake of simplicity, let the electron wave function associated with the quantized z motion be

$$\xi_0(z)=\left[\frac{2}{a}\right]^{1/2}\cos\left[\frac{\pi}{a}z\right]\quad\text{for}\quad-\frac{1}{2}a\leq z\leq\frac{1}{2}a\ . \tag{3.21}$$

For this wave function which vanishes in the barrier layers, $F_{H+}(Q)$ and $F_{H-}(Q)$ are identically zero. Moreover, $F_A(Q)$ vanishes because of the symmetry. In Fig. 5 we show $F_C(Q)$ and $F_S(Q)$ as a function of Qa together with $F_B(Q)$ for comparison. The wavelength dependence shown in Fig. 5 is similar to that in the single heterostructure (Fig. 3). Contributions of interface phonons become more and more important for long wavelengths or in narrow wells, which is analogous to the case of single heterostructures considered in Sec. III A. However, there is an important difference: In case of single heterostructures, the coupling constants of interface phonons are independent of the momentum Q and the two interface phonons $\omega_\pm$ contribute to electron-phonon interactions. In the case of double heterostructures, on the other hand, one of $\alpha_{S\pm}(Q)$ (α_{S+} in Fig. 4) approaches α_2 and the other (α_{S-} in Fig. 4) vanishes in the limit of long wavelengths or narrow well widths. This means that electrons in a narrow quantum well interact only with LO phonons outside the well.

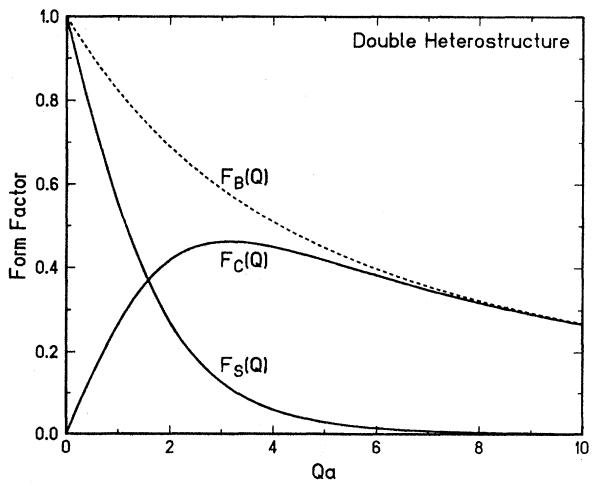

FIG. 5. The form factors in a double heterostructure, $F_S(Q)$ and $F_C(Q)$, as a function of Qa together with the form factor of bulk LO phonons, $F_B(Q)$. Since we use Eq. (3.21) as the wave function, $F_{H+}(Q)$, $F_{H-}(Q)$, and $F_A(Q)$ are identically zero, and $F_S(Q)+F_C(Q)=F_B(Q)$.

IV. POLARON MOBILITY

For the sake of the simplicity, we will consider the interaction of just a single electron with optical phonons and the low-field mobility of electrons to the lowest order in coupling constants. The mobility μ limited by scatterings from optical phonons is given by

$$\mu = e\tau_p / m^* , \tag{4.1}$$

where $\tau_p = (2\Gamma_{\rm tot})^{-1}$ is the total scattering time with the total polaron damping rate $\Gamma_{\rm tot}$, which is the sum of Γ_j associated with mode j over all the modes.

We calculate the polaron damping rate as the imaginary part of the self-energy in small wave-vector limit and have[13]

$$\Gamma_j(k \ll \gamma_j) = \frac{\pi}{2} \left[\frac{1}{|1-\omega_j'(\gamma_j)/E'(\gamma_j)|} \right] \alpha_j(\gamma_j)\omega_j(\gamma_j) \times N_B(\omega_j(\gamma_j))F_j(\gamma_j) , \tag{4.2}$$

where k is the magnitude of electron wave vector, $E(k)$ is the electron energy $E(k)=k^2/2m^*$, $N_B(\omega)$ is a distribution function for optical phonons with frequency ω, γ_j is a solution of $E(\gamma_j)=\omega_j(\gamma_j)$ $(\gamma_j>0)$, i.e., the wave vector which satisfies both energy- and momentum-conservation law, $E'(k)=\partial E(k)/\partial k$, and $\omega_j'(Q)=\partial\omega_j(Q)/\partial Q$. The term within the large parentheses is identically unity for half-space phonons or confined phonons. Further, its deviation from unity for interface phonons is usually unimportant because $\omega_j'(\gamma_j)/E'(\gamma_j)$ is at most of the order of $(\omega_{Ln}-\omega_{Tn})/2\omega_{Ln}$ which is much smaller than unity for most semiconductors.

A. GaAs/AlAs single heterostructures

The polaron damping rate Γ_j is determined by the optical phonons whose wave vector parallel to the interface is γ_j. The amplitude of the interface phonons decreases exponentially away from the interface according to $\exp(-\gamma_j|z|)$. Therefore, if the average distance between electrons and the interface $z_{\rm av}$ is larger than γ_j^{-1} (i.e., $z_{\rm av}\gamma_j > 1$), effects of the interface phonons become negligibly small and we can safely use the usual bulk Fröhlich Hamiltonian. On the other hand, if $z_{\rm av}\gamma_j < 1$, we cannot neglect the effect of the interface phonons as well as the reduction of that of the half-space LO phonons.

We calculate Γ_j in a GaAs/AlAs single heterostructure using the Fang-Howard trial function Eq. (3.10). The results are shown in Fig. 6 as a function of $N^*=N_{\rm depl}+\frac{11}{32}N_s$, where $N_{\rm depl}$ is the depletion charge density and N_s is the electron sheet density, together with the damping rate Γ_B obtained by assuming bulk GaAs LO phonons. The damping rates are normalized by $\Gamma_0^{(1)}=\frac{1}{2}\pi\alpha_1\omega_{L1}N_B(\omega_{L1})$, which is that of an ideal two-dimensional electron gas, i.e., $|\xi_0(z)|^2=\delta(z)$, in bulk GaAs. In GaAs/AlAs single heterostructures, $z_{\rm av}\sim 3/b\sim 110$ Å (for $N^*=1.5\times10^{11}$ cm^{-2}), $\gamma_j^{-1}\sim\gamma_{L1}^{-1}\sim 40$ Å [where $\gamma_{L1}=(2m^*\omega_{L1})^{1/2}$], and $z_{\rm av}\gamma_j\sim 2.8$, which shows that we can neglect the effect of the interface phonons as actually demonstrated in Fig. 6.

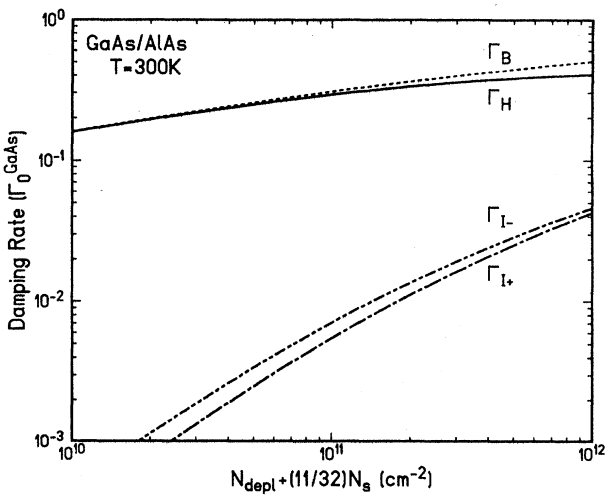

FIG. 6. The polaron damping rates in a GaAs/AlAs single heterostructure as a function of $N^*=N_{\rm depl}+\frac{11}{32}N_s$ at $T=300$ K. Γ_H is for half-space phonons in the right half-space, Γ_{I+} (Γ_{I-}) is for interface phonons ω_+ (ω_-). Γ_B is the damping rate for bulk phonons. The average distance between electrons and the interface is so large that the contribution of interface phonons can be neglected and there is no notable difference between Γ_H and Γ_B.

B. AlAs/GaAs/AlAs double heterostructures

In Fig. 7 we show Γ_j in an AlAs/GaAs/AlAs heterostructure as a function of well width a. We consider intrasubband transitions within the ground subband only, and use Eq. (3.21) as the electron wave function along the

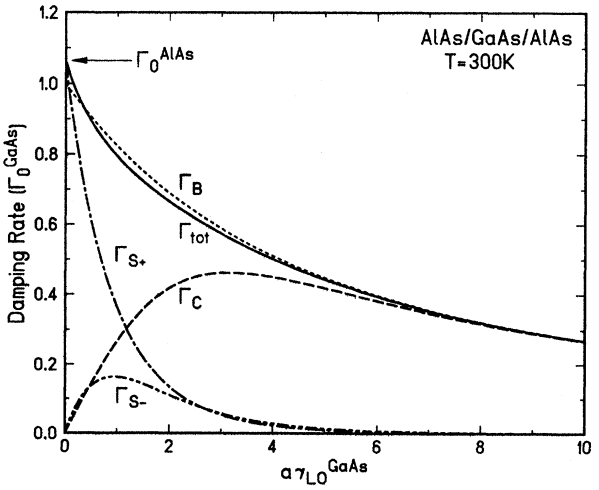

FIG. 7. The polaron damping rates in an AlAs/GaAs/AlAs double heterostructure as a function of $\gamma_{L1}a$ at $T=300$ K. Γ_C is for confined phonons, Γ_{S+} (Γ_{S-}) is for symmetric interface phonons ω_{S+} (ω_{S-}), and $\Gamma_{\rm tot}$ is the total rate, i.e., $\Gamma_{\rm tot}=\Gamma_C+\Gamma_{S+}+\Gamma_{S-}$. Γ_B is for bulk LO phonons. For thin wells such that $\gamma_{L1}a<1$, the contribution of interface phonons increases resulting in the reduction of the contribution of confined phonons. Because $\Gamma_0^{(1)}\sim\Gamma_0^{(2)}$, however, there is no notable difference between $\Gamma_{\rm tot}$ and Γ_B.

z axis. Note that LO-phonon absorption due to intersubband transitions can occur for wells wider than $\pi\sqrt{3}\gamma_{L1}^{-1}$ (i.e., $\gamma_{L1}a > \pi\sqrt{3} \sim 5.4$).

When the well width decreases ($\gamma_{L1}a \lesssim 6$), the contribution of modes confined in the well starts to decrease and those of symmetric interface phonons ω_{S+} and ω_{S-} become appreciable. With further decrease of the width, the contribution of ω_{S+}, which approaches the LO phonon in the barrier ω_{L2}, continues to rise. The contributions of ω_{S-}, on the other hand, has a maximum and then starts to decrease. This is because ω_{S-} approaches ω_{T1}, the TO phonon in the well, as has been mentioned in the preceding section. This crossover occurs around $\gamma_{L1}a=1$. In the limit of thin well widths ($\gamma_{L1}a \to 0$), the total damping rate Γ_{tot} converges to $\Gamma_0^{(2)} = \frac{1}{2}\pi\alpha_2\omega_{L2}N_B(\omega_{L2})$, that of an ideal two-dimensional electron gas in the barrier (with electron effective mass in the well). In AlAs/GaAs/AlAs systems, however, there exists only a small difference between $\Gamma_0^{(1)}$ and $\Gamma_0^{(2)}$ ($\Gamma_0^{(1)}=1.3$ meV and $\Gamma_0^{(2)}=1.4$ meV at $T=300$ K), and Γ_{tot} is not remarkably different from Γ_B.

C. AlSb/InAs/AlSb double heterostructures

The relevant physical parameters for AlSb/InAs/AlSb double heterostructures are $\omega_{L1}=30.2$ meV, $\omega_{T1}=27.1$ meV, $\kappa_{\infty 1}=12.3$, $\omega_{L2}=42.2$ meV, $\omega_{T2}=39.5$ meV, $\kappa_{\infty 2}=10.2$, and $m^*=0.023m_0$. We have $\alpha_1=0.050$ and $\alpha_2=0.032$, which leads to $\Gamma_0^{(1)} > \Gamma_0^{(2)}$. Because the effective mass of InAs is lighter than that of GaAs, the relation $\gamma_{L1}a<1$ is more easily satisfied ($\gamma_{L1}=1/74$ Å). Further, this system has a large barrier height for electrons [1.8 eV (Ref. 56)] which is advantageous in applications.

In Fig. 8 we show the damping rates as a function of well width. The damping Γ_{tot} is close to Γ_B and increases as decreasing well width for $\gamma_{L1}a>1$. However,

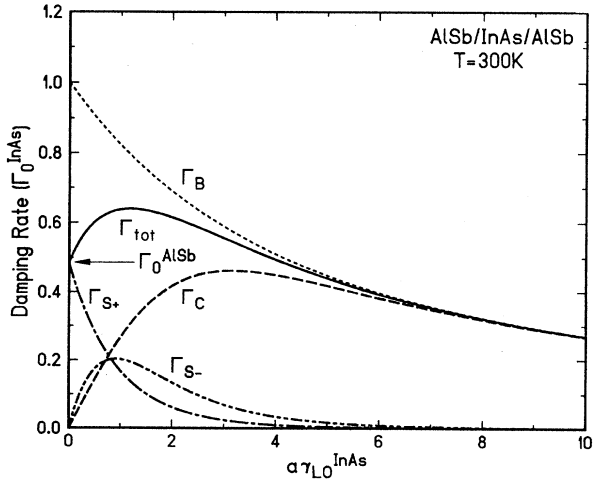

FIG. 8. The polaron damping rates in an AlSb/InAs/AlSb double heterostructure as a function of $\gamma_{L1}a$ at $T=300$ K. In this system, $\Gamma_0^{(1)}$ is larger than $\Gamma_0^{(2)}$, leading to the reduction of Γ_{tot} relative to Γ_B for thin wells.

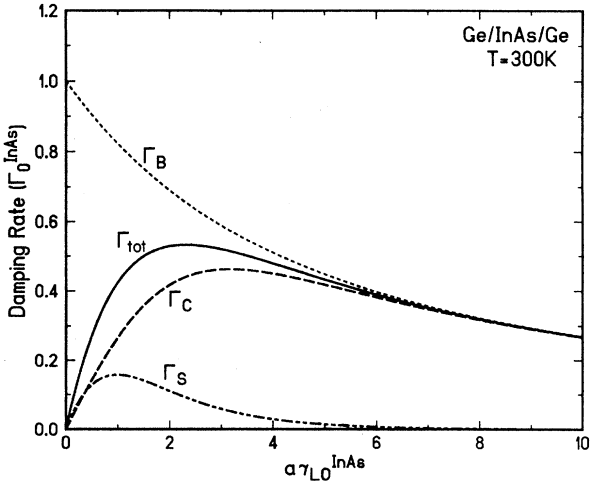

FIG. 9. The polaron damping rates in a Ge/InAs/Ge double heterostructure as a function of $\gamma_{L1}a$ at $T=300$ K. We have $\Gamma_{tot}=\Gamma_C+\Gamma_S$. Since Ge is homopolar, the notable reduction of Γ_{tot} occurs for the well widths such that $\gamma_{L1}a<1$, and Γ_{tot} approaches zero in the limit of vanishing width.

when the well width a becomes thinner than γ_{L1}^{-1}, Γ_{tot} starts to decrease in contrast to Γ_B. In the limit of infinitely narrow widths, Γ_{tot} converges to $\Gamma_0^{(2)}=0.52$ meV which is smaller than $\Gamma_0^{(1)}=1.1$ meV.

D. Ge/InAs/Ge double heterostructures

If the two-dimensional electron gas is formed in a homopolar-polar-homopolar heterostructure, we can expect that the polaron damping vanishes for the limit of thin well widths. To demonstrate this we will consider a Ge/InAs/Ge double heterostructure, in which two-dimensional electrons are confined in the InAs layer. The barrier height for electrons is estimated as 0.8 eV from the difference of electron affinities.[57] The relevant physical parameters are $\omega_{L1}=30.2$ meV, $\omega_{T1}=27.1$ meV, $\kappa_{\infty 1}=12.3$, $\omega_{L2}=37.3$ meV, $\kappa_{\infty 2}=15.8$, and $m^*=0.023m_0$. The frequency ω_S of symmetric interface phonons is given by Eq. (2.11) with $\epsilon_2=\kappa_{\infty 2}$ and its coupling constant is given by Eq. (3.11) with $\beta_2^{-1}=0$.

In Fig. 9, Γ_j's are shown as a function of the well width. In the limit of thin well widths, Γ_{tot} converges to zero as expected. The well-width dependence given in Fig. 9 is in qualitative agreement with the result of Riddoch and Ridley,[29] who have calculated the electron scattering rates as a function of electron energy in thin ionic (GaAs) slabs by utilizing the eigenmodes obtained by Fuchs and Kliewer[38] and found that the scattering rates can be significantly less than in the bulk.

V. MAGNETOPHONON RESONANCE

The magnetophonon resonance is an oscillation of the transverse magnetoresistance caused by resonant electron scatterings between Landau levels due to emissions and absorptions of optical phonons.[58,59] If we use the magne-

tophonon resonance, we can get much richer information about the electron–optical-phonon interaction in heterostructures.

Making a perturbation expansion of the Kubo formula for conductivity and taking into account broadening of Landau levels as a Lorentz form, we get the transverse magnetoconductivity $\sigma_{xx}^{(j)}$ corresponding to inelastic scatterings with the optical phonon (mode j) as[60,61,18,19]

$$\sigma_{xx}^{(j)}=\sum_{N,N'}\int_0^{+\infty}d\zeta\,\sigma_0^{(j)}(Q)\sqrt{\zeta}J_{NN'}^2(\zeta)F_j(Q)\times[f(E_N-\omega_j)-f(E_N)]\times\delta_\gamma((E_{N'}+\omega_j-E_N)/\omega_c)\,, \tag{5.1}$$

with

$$\sigma_0^{(j)}=\tfrac{1}{2}e^2\alpha_j(Q)\left[\frac{\omega_j(Q)}{\omega_c}\right]^{3/2}(\omega_c/T)N_B(\omega_j)\times[N_B(\omega_j)+1]\,, \tag{5.2}$$

where $\zeta=\frac{1}{2}Q^2l^2$ with l the cyclotron radius, ω_c is the cyclotron frequency, E_N is the Nth Landau-level energy, T is temperature, $f(E)$ is the Fermi-Dirac distribution function, $\delta_\gamma(x)$ is a Lorentzian function defined by $\delta_\gamma(x)=(\gamma/\pi)/(x^2+\gamma^2)$ with $\gamma=2\Gamma/\omega_c$ (Γ is the Landau-level width), and $J_{NN'}^2(\zeta)$ is the well-known matrix elements.[60,61] In the regime of high magnetic fields such as $\omega_c\tau\gg1$ (τ is the electron relaxation time), the transverse magnetoresistivity ρ_{xx} is proportional to σ_{xx}, i.e., $\rho_{xx}=\sigma_{xx}/(N_se^2/m^*\omega_c)^2$.

A. GaAs/AlAs single heterostructures

In Fig. 10 we show an example of calculated magnetoresistance spectra in a GaAs/AlAs single heterostructure. It clearly shows that contributions of the interface phonons are negligibly small in complete agreement with the case of the polaron damping rate. This is because the average distance between electrons and the interface is too large for interface phonons to contribute to ρ_{xx} appreciably.

There have been reported several experiments on magnetophonon resonances in GaAs/$Al_xGa_{1-x}As$ single heterostructures. Most of them have been explained in terms of bulk GaAs LO phonons[43–45,54] in agreement with the present calculations. However, some experiments have suggested that phonon frequencies are significantly lower than that of bulk GaAs LO phonons.[49,50,62] Experiments have been performed also in $In_xGa_{1-x}As/In_yAl_{1-y}As$ and $In_xGa_{1-x}As/InP$ heterostructures.[59] In $In_xGa_{1-x}As/In_yAl_{1-y}As$, electrons seem to interact mainly with InAs-like LO modes, while both in bulk GaInAs and in $In_xGa_{1-x}As/InP$, GaAs-like LO modes are dominant. Origins of these interesting experimental results remain unanswered.

B. AlAs/GaAs/AlAs double heterostructures

In Fig. 11, we show examples of calculated magnetoresistance spectra in AlAs/GaAs/AlAs double heterostructures with well width $a=100$ Å ($\gamma_{L1}a=2.5$), $a=50$ Å ($\gamma_{L1}a=1.3$), and $a=25$ Å ($\gamma_{L1}a=0.63$). In spite of the fact $\Gamma_0^{(1)}\sim\Gamma_0^{(2)}$ there appears a significant difference in the spectra of magnetophonon resonances. That interface phonons can be important in magnetophonon resonances in narrow quantum wells has been suggested by Lassnig[27] and Lassnig and Zawadzki[19] without any explicit calculations. They derived the Hamiltonian describing electron–optical-phonon interactions by application of a modified image-charge ansatz and calculated *form factors* (which correspond to the quantities $\alpha_j(Q)F_j(Q)/\alpha_n$ in the present paper) approximately. Although their derivation of the interaction Hamiltonian is based on the ansatz that is not justified, the resulting Hamiltonian seems to be identical with ours.

There have been experiments in InP/$In_xGa_{1-x}As$/InP double heterostructures,[46] which have shown that InAs-like modes are stronger in thicker wells ($a\sim100$ and 150 Å) while InP-like modes are more important in thinner wells ($a\sim80$ Å). If sample parameters appropriate in these systems are used, we have $\gamma_{L1}a\sim1.7$ for $a\sim80$ Å, where contributions from interface phonons to scatterings are already comparable to those from confined phonons according to the present calculation. Therefore, these experimental results can be explained qualitatively. Similar experiments in systems with well widths much narrower or wider than the above are required to observe a clear crossover of phonon modes dominant in electron scatterings.

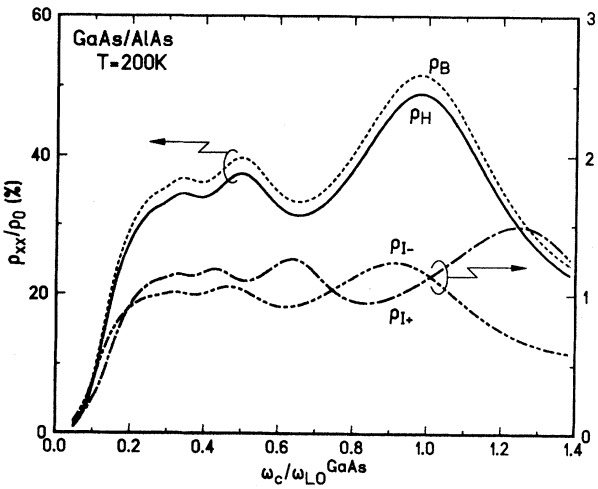

FIG. 10. The transverse magnetoresistivity ρ_{xx} as a function of ω_c/ω_{L1} of a GaAs/AlAs single heterostructure caused by magnetophonon resonances for $T=200$ K, $N_s=3\times10^{11}$ cm^{-2}, and $N_{depl}=5\times10^{10}$ cm^{-2}. The broadening of Landau levels Γ is 5 meV independent of the magnetic field. ρ_{xx} is normalized by $\rho_0=2m^*\Gamma_0^{(1)}/N_se^2$. ρ_{I+} (ρ_{I-}) is for interface phonons ω_{I+} (ω_{I-}), ρ_H for half-space phonons in right half-space, and ρ_B for bulk phonons. The average distance between electrons and the interface is so large that $\rho_{I\pm}$ is negligibly small relative to ρ_H and there is no notable difference between ρ_H and ρ_B.

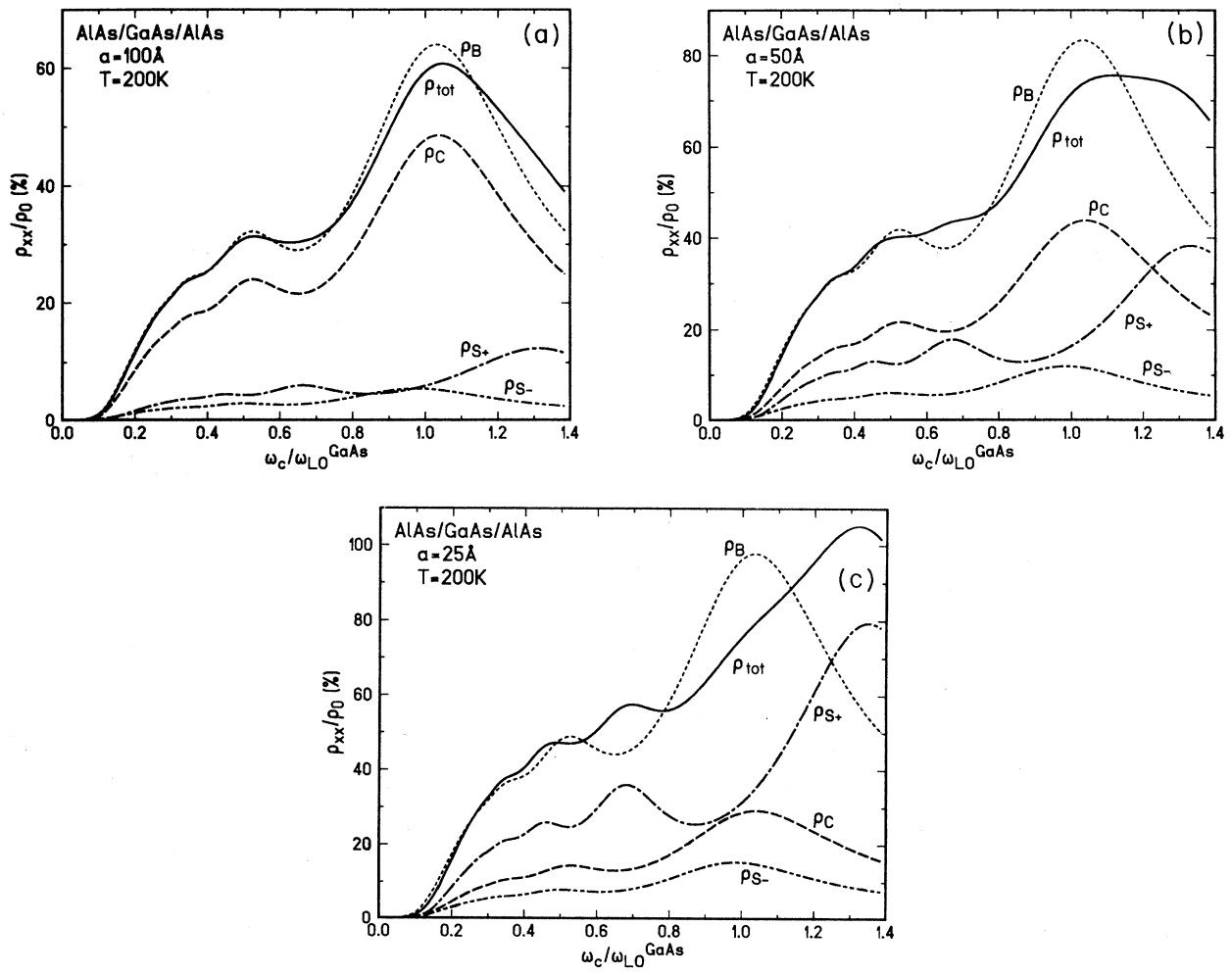

FIG. 11. The magnetoconductivity as a function of ω_c/ω_{L1} of an AlAs/GaAs/AlAs double heterostructure caused by magneto-phonon resonances for $T=200$ K, $N_s=1\times10^{12}$ cm^{-2}, and $\Gamma=5$ meV. ρ_{S+} (ρ_{S-}) is for symmetric interface phonons with frequency ω_{S+} (ω_{S-}), ρ_C for confined phonons, ρ_B for bulk phonons, and $\rho_{\rm tot}=\rho_{S+}+\rho_{S-}+\rho_C$. (a) $a=100$ Å ($\gamma_{L1}a=2.5$), (b) $a=50$ Å ($\gamma_{L1}a=1.3$), and (c) $a=25$ Å ($\gamma_{L1}a=0.63$).

VI. DISCUSSION AND CONCLUSION

We have derived in this paper the effective electron-electron interaction mediated by optical phonons in semiconductor single and double heterostructures. The Hamiltonian describing electron–optical-phonon interactions has been obtained using orthonormal eigenmodes of optical phonons calculated within the dielectric continuum model.

One of the important results is the *sum rule* of form factors, Eqs. (3.8) and (3.20), which states that the sum of the contributions of all kinds of phonon modes is exactly equal to that of bulk modes if coupling constants are independent of modes. This leads to a certain relation between the contribution of interface phonons and that of the rest (half-space LO phonons in single heterostructures, confined LO phonons in double heterostructures and so on). That is, the reduction of interactions with confined LO phonons (or half-space LO phonons) does not necessarily mean the reduction of the *total* interaction because of the increase of interactions with interface phonons. In double heterostructures we have found that electrons confined in the well interact mainly with phonons of barrier layers in narrow wells such that $\gamma_{L1}a<1$. Therefore, we can reduce the total electron–optical-phonon interaction by using thin ionic slabs as suggested by Riddoch and Ridley[29] or the double heterostructures such that $\Gamma_0^{(1)}>\Gamma_0^{(2)}$, especially the homopolar-polar-homopolar double heterostructures, as discussed in this paper.

In AlAs/GaAs single heterostructures, we have found that the contribution of the interface phonons can be neglected as compared with that of half-space LO phonons. Note that this does not mean that interface phonons are completely neglected in single heterostructures. If we consider phenomena where phonons with long

wavelengths play dominant roles, for example, resonant polaron couplings in magnetic fields, there can be appreciable contributions of interface phonons. Usually resonant polaron couplings give rise to a discontinuity in the effective mass when $\omega_c \sim \omega_j$. The discontinuities at interface phonons ω_+ and ω_- are estimated as about $\frac{1}{4}$ of that at ω_{L1}. There have been no experiments which have observed such discontinuities occurring at frequencies of interface phonons in $GaAs/Al_xGa_{1-x}As$ systems.[62] It may be hard to observe the discontinuity at ω_- as ω_- is close to ω_{L1} while that at ω_+ may be observed more easily. In double heterostructures with narrow well widths we can expect stronger discontinuities at the frequency of interface phonons. Resonant polaron effects have been observed in $In_xGa_{1-x}As/In_yAl_{1-y}As$ and $In_xGa_{1-x}As/InP$ heterostructures, where discontinuities in the effective mass look similar to those occurring at the GaAs- and InAs-like TO phonons.[63,64] This has not been explained satisfactorily although there have been attempts to ascribe it to interface phonons[65] or plasmon-phonon couplings[66] without explicit calculations.

The present study is restricted to the case of heterostructures composed of diatomic semiconductors in spite of the fact that most experiments have been carried out in systems consisting of alloy semiconductors. In the case of alloys, it is not possible to obtain exact phonon modes possessing complete orthonormality because of the presence of randomness and we have to introduce some approximations. In case of alloys with well-separated two modes, the present calculation can easily be extended by using the generalized Lyddane-Sachs-Teller relations[59] to determine the coupling constant for each mode. It may be possible to use the image-charge ansatz,[27] because we now know that it gives the effective electron-electron interactions identical with that obtained in the present method in the single-mode case.

It may be worthwhile to make a few remarks on the dielectric continuum model. There have been various calculations reported of phonon modes in superlattices.[67–74] Such calculations have shown that phonon eigenmodes, though quite complicated, can be different from those predicted in the dielectric continuum model especially in the vicinity of interfaces. Further, there can be interface localized modes whose origins are quite different from those discussed in this paper. It is expected, however, that the dielectric continuum model can still give reasonable answers to various problems in single heterostructures and wide quantum wells (meaning much wider than the lattice constant), since such perturbations due to the presence of interfaces seem to be localized within a few atomic layers from interface planes. In order to give a definite answer to the accuracy of the dielectric continuum model, we have to perform more elaborate calculations using phonon eigenmodes obtained by lattice dynamics or other reliable methods.[73,74] This problem is certainly out of the scope of the present paper and left for future study.

ACKNOWLEDGMENTS

One of the authors (N.M.) wishes to thank Professor C. Hamaguchi for his encouragement and Dr. H. Akera for helpful discussions. This work was carried out under the auspices of the Institute for Solid State Physics, the University of Tokyo. This work is supported in part by a Grant-in-Aid for specially promoted research from the Ministry of Education, Science and Culture, Japan.

[1]D. K. Ferry, Surf. Sci. **75**, 86 (1978).
[2]K. Hess, Appl. Phys. Lett. **35**, 484 (1979).
[3]P. J. Price, Ann. Phys. (N.Y.) **133**, 217 (1981); Surf. Sci. **113**, 199 (1982); Phys. Rev. B **30**, 2234 (1984).
[4]T. J. Drummond, H. Morkoç, K. Hess, and A. Y. Cho, J. Appl. Phys. **52**, 5231 (1981).
[5]B. K. Ridley, J. Phys. C **15**, 5899 (1982).
[6]F. A. Riddoch and B. K. Ridley, J. Phys. C **16**, 6971 (1983).
[7]K. Lee, M. S. Shur, T. J. Drummond, and H. Morkoç, J. Appl. Phys. **54**, 6432 (1983).
[8]W. Walukiewicz, H. E. Ruda, J. Lagowski, and H. C. Gatos, Phys. Rev. B **30**, 4571 (1984).
[9]B. A. Mason and S. Das Sarma, Phys. Rev. B **35**, 3890 (1987).
[10]S. Das Sarma, Phys. Rev. Lett. **52**, 859 (1984).
[11]D. M. Larsen, Phys. Rev. B **30**, 4807 (1984).
[12]F. M. Peeters and J. T. Devreese, Phys. Rev. B **31**, 3689 (1985).
[13]S. Das Sarma and B. A. Mason, Ann. Phys. (N.Y.) **163**, 78 (1985).
[14]B. A. Mason and S. Das Sarma, Phys. Rev. B **35**, 3890 (1987), and references cited therein.
[15]X.-G. Wu, F. M. Peeters, and J. T. Devreese, Phys. Rev. B **34**, 8800 (1986); **36**, 9765 (1978); F. M. Peeters, X.-G. Wu, and J. T. Devreese, Surf. Sci. **196**, 437 (1988).
[16]M. H. Degani and O. Hipólito, Phys. Rev. Lett. **59**, 2820 (1987).
[17]S. Das Sarma, J. K. Jain, and R. Jalabert, Phys. Rev. B **37**, 1228 (1988).
[18]R. Lassnig and W. Zawadzki, J. Phys. C **16**, 5435 (1983).
[19]R. Lassnig and W. Zawadzki, Surf. Sci. **142**, 361 (1984).
[20]M. P. Chaubey and C. M. V. Vliet, Phys. Rev. B **33**, 5617 (1986).
[21]P. Vasilopoulos, Phys. Rev. B **33**, 8587 (1986).
[22]N. Mori, H. Murata, K. Taniguchi, and C. Hamaguchi, Phys. Rev. B **38**, 7622 (1988).
[23]P. Vasilopoulos, M. Charbonneau, and C. M. Van Vliet, Phys. Rev. B **35**, 1334 (1987).
[24]P. Warmenbol, F. M. Peeters, and J. T. Devreese, Solid-State Electron. **31**, 771 (1988).
[25]P. Warmenbol, F. M. Peeters, and J. T. Devreese, Phys. Rev. B **37**, 4694 (1988).
[26]M. V. Klein, IEEE J. Quantum Electron. **QE-22**, 1760 (1986).
[27]R. Lassnig, Phys. Rev. B **30**, 7132 (1984).
[28]B. K. Ridley, in *Festkörperprobleme*, edited by H. J. Quiesser (Vieweg, Braunschweig, 1985), Vol. XXV, p. 449.
[29]F. F. Riddoch and B. K. Ridley, Physica B+C **134B**, 342 (1985).
[30]N. Sawaki, Surf. Sci. **170**, 537 (1986).
[31]N. Sawaki, J. Phys. C **19**, 4965 (1986).
[32]C. T. Giner and F. Comas, Phys. Rev. B **37**, 4583 (1988).

[33]M. H. Degani and O. Hipólito, Phys. Rev. B **35**, 7717 (1987).
[34]M. H. Degani and O. Hipólito, Surf. Sci. **196**, 459 (1988).
[35]S.-W. Gu, X.-J. Kong, and C.-W. Wei, Phys. Rev. B **36**, 7977 (1987).
[36]C.-W. Wei, X.-J. Kong, and S.-W. Gu, Phys. Rev. B **38**, 8390 (1988).
[37]S.-W. Gu, Y.-C. Li, and L.-F. Zheng, Phys. Rev. B **39**, 1346 (1989).
[38]R. Fuchs and K. L. Kliewer, Phys. Rev. **140**, A2076 (1965).
[39]A. A. Lucas, E. Kartheuser, and R. G. Badro, Phys. Rev. B **2**, 2488 (1970).
[40]J. J. Licari and R. Evrard, Phys. Rev. B **15**, 2254 (1977).
[41]E. P. Pokatilov and S. I. Beril, Phys. Status Solidi B **118**, 567 (1983).
[42]L. Wendler, Phys. Status Solidi B **129**, 513 (1985).
[43]D. C. Tsui, Th. Englert, A. Y. Cho, and A. C. Gossard, Phys. Rev. Lett. **44**, 341 (1980).
[44]Th. Englert, D. C. Tsui, J. C. Portal, J. Beerens, and A. C. Gossard, Solid State Commun. **44**, 1301 (1982).
[45]G. Kido, N. Miura, H. Ohno, and H. Sakaki, J. Phys. Soc. Jpn. **51**, 2168 (1982).
[46]J. C. Portal, J. Cisowski, R. J. Nicholas, M. A. Brummell, M. Razeghi, and M. A. Poisson, J. Phys. C **16**, L573 (1983).
[47]M. A. Brummell, R. J. Nicholas, J. C. Portal, K. Y. Cheng, and A. Y. Cho, J. Phys. C **16**, L579 (1983).
[48]J. C. Portal, G. Grégoris, M. A. Brummell, R. J. Nicholas, M. Razeghi, M. A. di Forte–Poisson, K. Y. Cheng, and A. Y. Cho, Surf. Sci. **142**, 368 (1984).
[49]M. A. Brummell, R. J. Nicholas, M. A. Hopkins, J. J. Harris, and C. T. Foxon, Phys. Rev. Lett. **58**, 77 (1987).
[50]M. A. Brummell, D. R. Leadley, R. J. Nicholas, J. J. Harris, and C. T. Foxon, Surf. Sci. **196**, 451 (1988).
[51]N. Mori, K. Taniguchi, C. Hamaguchi, S. Sasa, and S. Hiyamizu, J. Phys. C **21**, 1791 (1988).
[52]G. Grégoris, J. Beerens, S. Ben Amor, L. Dmowski, J. C. Portal, F. Alexandre, D. L. Sivco, and A. Y. Cho, Phys. Rev. B **37**, 1262 (1988).
[53]D. R. Leadley, M. A. Brummell, R. J. Nicholas, J. J. Harris, and C. T. Foxon, Solid-State Electron. **31**, 781 (1988).
[54]P. Hawker, A. J. Kent, L. J. Challis, M. Henini, and O. H. Hughes, J. Phys. Condens. Matter **1**, 1153 (1989).
[55]F. F. Fang and W. E. Howard, Phys. Rev. Lett. **16**, 797 (1966); F. Stern and W. E. Howard, Phys. Rev. **163**, 816 (1967).
[56]L. F. Luo, R. Beresford, and W. I. Wang, Appl. Phys. Lett. **53**, 2320 (1988).
[57]H. Kressel and J. K. Butler, in *Semiconductor Lasers and Heterojunction LED's* (Academic, New York, 1979), Vol. 14, pp. 66–192.
[58]R. J. Nicholas, Prog. Quantum Electron. **10**, 1 (1985).
[59]R. J. Nicholas, M. A. Brummell, and J. C. Portal, in *Two-Dimensional Systems, Heterostructures, and Superlattices,* edited by G. Bauer, F. Kuchar, and H. Heinrich (Springer-Verlag, Berlin, 1984), p. 69.
[60]R. Kubo, S. J. Miyake, and N. Hashitsume, in *Solid State Physics,* edited by F. Seitz and D. Turnbull (Academic, New York, 1965), Vol. 17, p. 279.
[61]J. R. Barker, J. Phys. C **5**, 1657 (1972).
[62]C. J. G. M. Langerak, J. Singleton, P. J. van der Wel, J. A. A. J. Perenboom, D. J. Barnes, R. J. Nicholas, M. A. Hopkins, and C. T. Foxon, Phys. Rev. B **38**, 13 133 (1988).
[63]R. J. Nicholas, L. C. Brunel, S. Huant, K. Karrai, J. C. Portal, M. A. Brummell, M. Razeghi, K. Y. Cheng, and A. Y. Cho, Phys. Rev. Lett. **55**, 883 (1985).
[64]L. C. Brunel, S. Huant, R. J. Nicholas, M. A. Hopkins, M. A. Brummell, K. Karrai, J. C. Portal, M. Razeghi, K. Y. Cheng, and A. Y. Cho, Surf. Sci. **170**, 542 (1986).
[65]S. Das Sarma, Phys. Rev. Lett. **57**, 651 (1986).
[66]R. Lassnig, Surf. Sci. **170**, 549 (1986).
[67]S. K. Yip and Y. C. Chang, Phys. Rev. B **30**, 7037 (1984).
[68]E. Molinari, A. Fasolino, and K. Kunc, Phys. Rev. Lett. **56**, 1751 (1986); in *Proceedings of the 18th International Conference on the Physics of Semiconductors, Stockholm, 1986,* edited by O. Engström (World Scientific, Singapore, 1987), Vol. 1, p. 663.
[69]T. Toriyama, N. Kobayashi, and Y. Horikoshi, Jpn. J. Appl. Phys. **25**, 1895 (1986).
[70]E. Richter and D. Strauch, Solid State Commun. **64**, 867 (1987).
[71]S. F. Ren, H. Chu, and Y. C. Chang, Phys. Rev. Lett. **59**, 1841 (1987); Phys. Rev. B **37**, 8899 (1988).
[72]H. Chu, S. F. Ren, and Y. C. Chang, Phys. Rev. B **37**, 10 746 (1988).
[73]T. Tsuchiya, H. Akera, and T. Ando, Phys. Rev. B **39**, 6025 (1989).
[74]H. Akera and T. Ando, Phys. Rev. B **40**, 2914 (1989).